Physica Medica (2010) **26**, 202–208

available at www.sciencedirect.com

ScienceDirect

journal homepage: http://intl.elsevierhealth.com/journals/ejmp

ORIGINAL PAPER

Influence of Geant4 parameters on dose distribution and computation time for carbon ion therapy simulation

Nabil Zahra [a,b,c,*], **Thibault Frisson** [a,b,c,d], **Loic Grevillot** [a,c,d,e], **Philippe Lautesse** [a,b], **David Sarrut** [a,c,d]

[a] *Université de Lyon, 69622 Lyon, France*
[b] *IPNL-CNRS/IN2P3 UMR 5822, Université Lyon1, Villeurbanne, France*
[c] *Centre de lutte contre le cancer Léon Berard, 28 rue Laennec, 69373 Lyon cedex 08, France*
[d] *Creatis LRMN-CNRS UMR 5220, INSERM U 630, INSA, Université Lyon 1, Villeurbanne, France*
[e] *IBA, Louvain-La-Neuve, Belgium*

Received 11 September 2009; received in revised form 17 November 2009; accepted 23 December 2009
Available online 27 January 2010

KEYWORDS
GEANT4;
Dosimetry;
Hadrontherapy;
Linear energy transfer

Abstract The aim of this work was to study the influence of Geant4 parameters on dose distribution and computational time for simulations of carbon ion therapy. The study was done using Geant4 version 9.0. The dose distribution in water for incident monoenergetic carbon ion beams of 300 MeV/u were compared for different values of secondary particle production threshold and different step limits. Variations of depth dose of about 2 mm were observed in some cases, which induced a 30% variation of dose deposit in the Bragg peak region. Other tests were done using Geant4 version 9.2 to verify the results from this study. The two versions provided converging results and led to the same conclusions.

Introduction

Geant4 is a popular toolkit, developed through an international collaboration, allowing to simulate the passage of particles through matter [1]. It is used in the field of hadrontherapy for the simulation of both proton [2] and carbon beams [3].

One of the principal features that characterize the passage of a charged particle through matter is the energy lost by the particle. This effect is the result of inelastic collision with atomic electrons of the material. This process is almost solely responsible for the energy loss of heavy particles in matter. Lost energy is transferred to the atom causing ionization (hard collision) or excitation (soft

* Corresponding author at: Centre de lutte contre le cancer Léon Bérard, service de Radiothérapie, 28 rue Laennec, 69 373 Lyon Cedex 08, France. Tel.: +33 4 78 78 51 51; fax: +33 4 78 78 59 98.
E-mail address: zahra@lyon.fnclcc.fr (N. Zahra).

1120-1797/$ - see front matter © 2010 Associazione Italiana di Fisica Medica. Published by Elsevier Ltd. All rights reserved.
doi:10.1016/j.ejmp.2009.12.001

collision). The particles produced by the fragmentation process also cause ionization in matter as illustrated by the Bragg peak tail, but this phenomenon will not be studied here.

In Geant4 each particle track is composed of many steps. Each step contains all information about particle interactions with matter. The ionization energy loss is calculated for each step using the Bethe-Bloch formula [4]. The particle energy loss E is divided into continuous energy loss and production of secondary electrons. The *production threshold* is defined as the minimum energy E_{cut} above which secondary particles will be produced and tracked. When $E < E_{cut}$, E is lumped into the continuous energy loss and when $E > E_{cut}$, secondary electrons are produced. In Geant4 this threshold is set as a range in millimeters, not in energy to avoid the dependence on particle type and material. With each range, depending on the material, a kinetic energy is associated. For electrons and positrons, the conversion from range to kinetic energy is done according to the *continuous slow down approximation* (c.s.d.a). The *c.s.d.a* range is obtained when angular straggling is very small [5]. This can be done by disabling the multiple scattering process and the generation of delta rays.

In Geant4, it is assumed that the step is small enough for cross sections to remain approximately constant during the step. In ionization processes, electron emission occurs at the end of each step. Hence, the step size depends on the production threshold. In principle, to respect the conditions of Geant4, one must use small step sizes and consequently small production thresholds, in order to insure accurate simulation but this drastically increases the computing time. Fig. 1 represents the number of electrons produced by a 300 MeV/u carbon ion in water for different production thresholds. We observe that the number of secondary electrons starts to become significant for production threshold values below 10^{-2} mm.

On the other hand, a Geant4 process can be used to limit the step size (named *step limiter*) until it appears small enough to fulfill the conditions for the cross section to be constant along the step. However, we cannot underestimate the importance of the number of secondaries produced for the calculation of the spatial dose distribution, even though calculation time increases. One should choose the best combination of both parameters (production thresholds and step limiter) allowing accurate simulation in terms of spatial dose distribution and reasonable computation time.

Dose deposition for therapeutic carbon ion beam estimated with Geant4 has been found to agree with measured data [3]. Likewise, we have done some experimental measurements to illustrate that depth dose deposition agrees with Geant4 simulation [6,7] and with the values recommended by the IAEA TRS-398 [8]. The results show a difference of approximately 5% between the measured and the calculated depth dose deposited [9]. Fig. 2 shows a comparison between Geant4 simulation and experiments of an irradiated radiochromic film at 60 Gy with the ^{12}C beam of 95 MeV/u.

We take as a reference the ranges given by the ICRU 73 for carbon ion in liquid water [5] where the mean excitation energy value is assumed to be equal to I = 67.2 eV. The tables of stopping forces given in the ICRU 73 report were computed by the PASS code [10]. In the used Geant4 version (9.0), we take I = 70.89 eV (the default value). However, there are still uncertainties about stopping forces, notably the mean excitation energy, as well as about projectile fragmentation and other energy loss mechanisms [11]. According to recent experiments performed at GSI [12], this value could be changed to I = 78 eV in the next 9.3 version. The uncertainties according to I seems large [11] but we are not going to study this parameter in this paper, so we decided not to change the default value in Geant4. This will not change the conclusions of this study because if the correct range for a light ion beam is known at one energy, one can use any code based on the Bethe theory of stopping power (such as Geant4) and adjust the mean excitation energy to obtain a good agreement between calculated range and measurement [13,14].

In this study, we aimed to evaluate the influence of Geant4 parameters on energy deposit distribution by carbon ions in the context of cancer therapy in order to achieve the spatial resolution of dose distribution required for radiotherapy. In the present study we propose various simulations to help users fix parameter values and understand their influence.

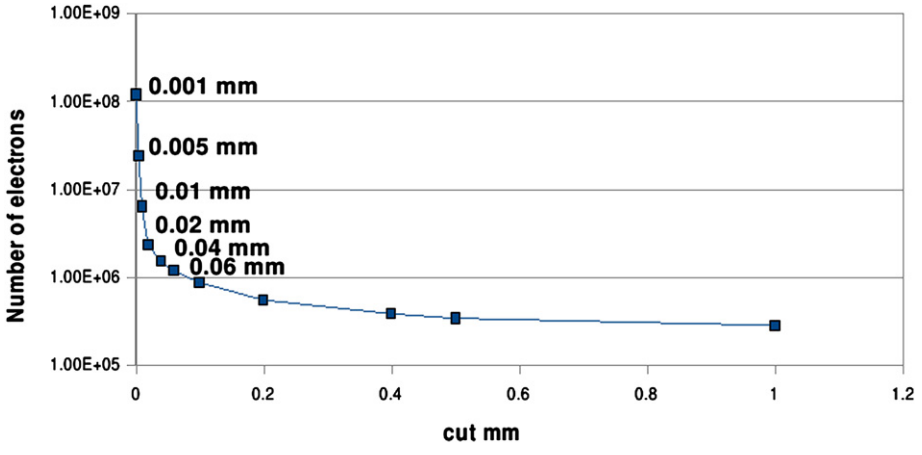

Figure 1 Number of secondary electrons produced for different production threshold values.

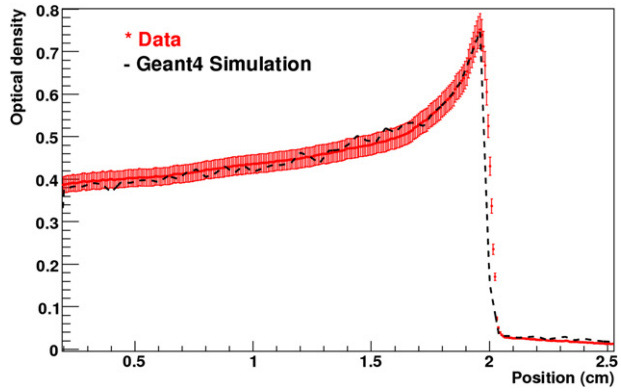

Figure 2 Measured net optical density using radiochromic film irradiated at 60 Gy with the ^{12}C beam as a function of the position along the *x* axis of the film (red dots). Error bars indicate the precision of measurements. The black dotted line is the optical density calculated by Geant4. Application method in [9]. (For interpretation of the references to colour in this figure legend, the reader is referred to the web version of this article).

Methods

Simulations were done with the GATE software based on Geant4 [1,4,15]. The tools used in this study will be included into the next public release of the GATE software (V6).

We simulated a box of water of $30 \times 30 \times 300$ mm^3 using Geant4 version 9.0. ''Dosels'' were defined as the scoring voxels of the scoring grid [16]. The dose deposit was stored in dosels of $30 \times 30 \times 0.5$ mm^3 attached to the water box. We used a fixed monoenergetic ^{12}C carbon ion beam with a square shape of 3×3 mm^2. We used the physics list QGSP_BIC_HP with the *Low Energy model* package that allows electron and photon simulations down to 250 eV. This model is used for medical applications [3] and was necessary for the study when using very low production threshold (10^{-3} mm). A detailed description of the physical models is given in the Physics Reference Manual [17]. Combinations of six production threshold values and six step size limit values were compared (see Table 1). The lowest parameters, a production threshold of 10^{-3} mm and a step limit of 10^{-2} mm, were chosen as references because they were considered to give the most accurate results and ranges consistent with the ICRU 73 report, with an error$\leq$ 1 mm (see Table 2).

Results

The depth dose deposition of an ion beam while it passes through matter is the most important characteristic for cancer treatment using hadrontherapy. As illustrated in Fig. 3, we plotted the depth dose profile for a production threshold of 1 mm without setting a limit on the step size (black crosses) as compared to the reference parameters (red dots). In this example, the mean statistical uncertainty was about 0.5%. We observed a 2 mm difference in the positions of the two Bragg peaks. Energy differences in the dose deposit could reach 30%. We have chosen three

Table 1 The different values of production thresholds and step limiter used in this study. The values in bold (red box) are the reference parameters.

Production Threshold (mm)	Step Limit (mm)
1	No Limits
0.5	2
0.1	1
0.01	0.1
0.005	0.05
0.001	**0.01**

criteria on which the evaluation of this study is based: dose deposit, computation time and local energy deposit.

Dose deposit

As seen in Fig. 3, a difference of about 30% in dose deposit as compared to the reference could be observed in some cases. The aim of the following criterion is to assess whether the difference in term of dose deposit in each dosel (0.5 mm in depth) compared to the reference situation is acceptable or not. In agreement with the dose discrepancy tolerated in conventional radiotherapy, we decided that the dose difference is acceptable if lower than 2%. Table 3 shows the number of dosels exceeding a 2% dose deposit difference as compared to the reference for each case. Fig. 4 illustrates the results obtained for a production threshold of 1 mm relatively to the reference. The section of the table where values do not meet this criterion can be disregarded. The differences are due to the under estimation of the energy loss while using too large step sizes and high production thresholds ($\geq$0.1 mm). The simulation does not meet the hypothesis that the cross sections are constant along the step and the corresponding parameters should be avoided.

Computation time

The Monte Carlo method is based on a stochastic approach, which makes it subject to statistical uncertainty. Many investigations have been performed to quantify the influence of statistical uncertainty on dose distribution [18,19]. In general the uncertainty is proportional to $1/\sqrt{N}$, where N is the number of simulated particles. Therefore, the

Table 2 Measured and calculted ranges for 3240 MeV (270 MeV/nucleon) C in water.

	c.s.d.a range (g/cm^2)
ICRU 73	14.19
Geant4	14.15

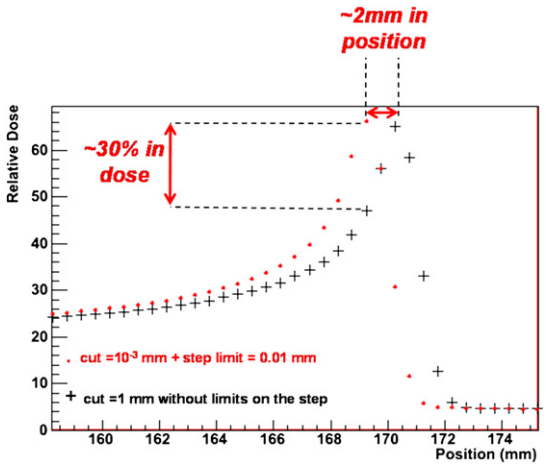

Figure 3 Difference of Bragg peak profile in two different cases. The red dot curve was obtained with the reference parameters and the black cross curve was obtained for a production threshold of 1 mm without setting a limit on the step. (For interpretation of the references to colour in this figure legend, the reader is referred to the web version of this article).

computation time increases with the number of particles. The mean uncertainty is obtained by averaging these quantities over all dosels.

$$I_{\text{mean}} = \frac{1}{n}\sum_{i=1}^{n}\sigma_i \qquad (1)$$

where n is the number of dosels, and σ_i the statistical uncertainty in dosel i as described for example in [18].

We defined the simulation time as the time needed to obtain 1% of mean statistical uncertainty. For that purpose, we computed and stored the uncertainties measured for increasing numbers of primary particles and we interpolated the number of primaries needed to reach exactly 1% (see Fig. 5). Table 4 shows the time required to reach 1% uncertainty relatively to the time required in the reference case. We observed that the lowest calculation time is obtained for a production threshold of 1 mm combined to a step size limit of 0.1 mm (in red); this is about 250 times faster (0.4%) than the reference case (in blue), for an equivalent dose distribution.

We used only 2500 primary particles with the reference parameters to reach 1% statistical uncertainty. The reference time (100%) was equivalent to 2 h 15 min on an Intel Xeon-3.00GHz. For the fastest simulation, it takes 60,000 particles to reach 1% uncertainty and it took less than 1 min. This difference is due to the different number of generated secondaries because of the different production thresholds.

Table 3 Number of points that exceed the 2% criterion on the dose deposited for each case.

Step mm / cut mm	No limit	2	1	0.1	0.05	0.01
1	132	69	37	0	0	0
0.5	63	54	32	0	0	0
0.1	8	8	8	0	0	0
0.01	0	0	0	0	0	0
0.005	0	0	0	0	0	0
0.001	0	0	0	0	0	0

Local energy deposit

To show the importance of small production thresholds for micro-dosimetry applications, we used the linear deposited energy (LDE), defined as the energy deposited along a track

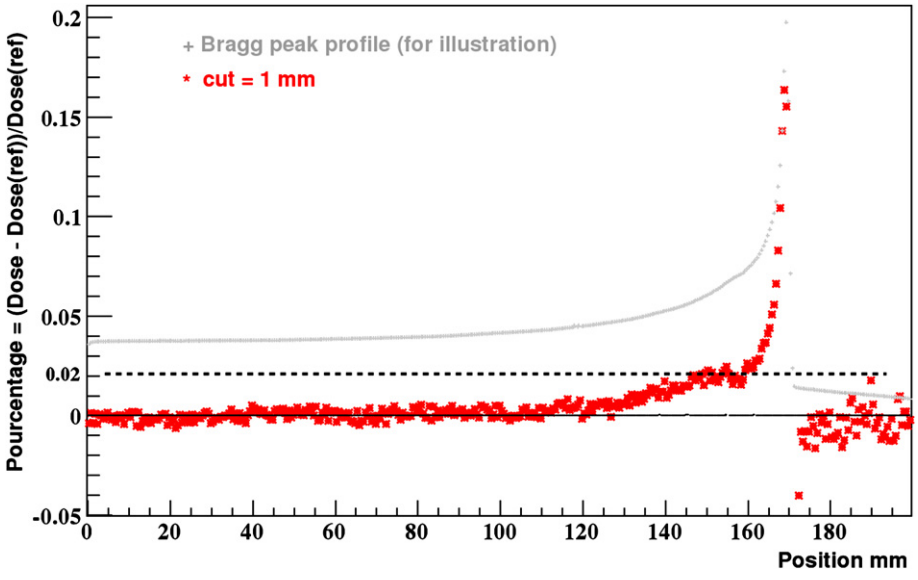

Figure 4 Percentage of dose difference along the Bragg peak profile relative to the reference for a production threshold of 1 mm. The red dot line illustrates the 2% criterion. The black dot line is obtained for a production threshold of 1 mm and the yellow dot line is for the reference production threshold of 10^{-3} mm. The Bragg peak profile (black dashes) is only for illustration. (For interpretation of the references to colour in this figure legend, the reader is referred to the web version of this article).

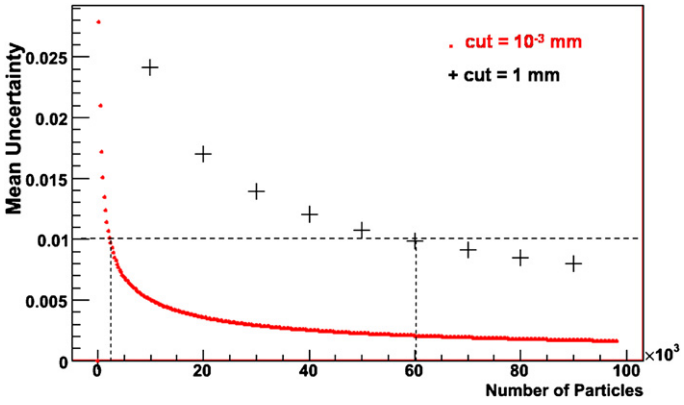

Figure 5 Mean statistical uncertainty as a function of the number of particles in two different cases: low production threshold = 10^{-3} mm (red dots) and high production thresholds = 1 mm (black crosses). (For interpretation of the references to colour in this figure legend, the reader is referred to the web version of this article).

segment divided by the length of the track segment. The LDE is similar to the linear energy transferred (LET) but LDE accounts for the deposited energy and not for the transferred energy. This criterion was used by [9]. We used a fixed step size limit of 0.1 mm and compared two different production thresholds, 1 mm and 10^{-3} mm. LDE values were compared for both values.

Fig. 6 shows a 2D histogram of the local energy deposited as a function of depth. Each entry corresponds to the number of steps at each position. We observed large differences in term of dose distribution along the whole Bragg peak curve. Indeed in Geant4, the energy deposited by a charged particle depends on the electron production threshold. In the case of high production threshold of 1 mm, the LDE count the energy of all the secondaries below the threshold, i.e. not produced, as an energy deposited continuously along the track of the primary particle. On the other hand, when using low production threshold of 10^{-3} mm, much more secondary electrons are produced and tracked, and the dose deposit distribution is better estimated. This makes the difference between the LDE distribution showed in Fig. 6.

In order to illustrate those finding with real-scaled case, we also computed the dose distribution inside a patient described from a CT image and compare 3D dose distributions with two different parameters sets. The situation becomes much more complicated in presence of inhomogeneities inside the body, rather than simply water [11] because composition of the human body plays an important role in interactions of heavy particles. We simulated a spread out Bragg peak ''SOBP'' in a head & neck patient's image. A cubic homogeneous ''tumor'' was inserted in the CT image of the head. We used a fixed step size limit of 0.1 mm and compared three different production thresholds: 1, 0.1 and 10^{-3} mm.

Fig. 7 shows the dose distribution in the target: sagittal view on the top right and coronal view on the bottom right. On the top left of the image we plotted the physical energy deposited in a given slice passing through the tumor (yellow rectangle in the image). The blue line represents the deposited energy obtained for the reference simulation (10^{-3} mm) and the triangles correspond to the energy obtained with production threshold of 1 mm. On the bottom left we show the difference in deposited energy relative to the reference. We observed that the production threshold value of 0.1 mm is consistent with the tolerated difference of 2% (see Section 3.1) in the plateau but differences could reach 8% in the Bragg peak tail due to the high dose gradient at the distal end. On the other hand, when using a high production threshold of 1 mm, differences in energy deposit along the Bragg peak could exceed the 2%. The large variation at the 43 mm position is due to the passage from air to cortical bone ''A''.

Table 4 Relative time needed to 1% mean statistically uncertainty.

Step mm / cut mm	No limit	2	1	0.1	0.05	0.01
1				0.38	0.66	2.80
0.5				0.40	0.67	2.64
0.1				0.90	1.14	2.83
0.01	6.51	6.24	6.30	6.36	6.48	7.43
0.005	21.26	21.68	22.02	22.92	22.89	22.69
0.001	96.82	98.41	97.16	99.53	99.04	100

New version of Geant4

When Geant4 is initialized, tables of linear energy loss are calculated (dE/dx). The Geant4.9.0 version calculated

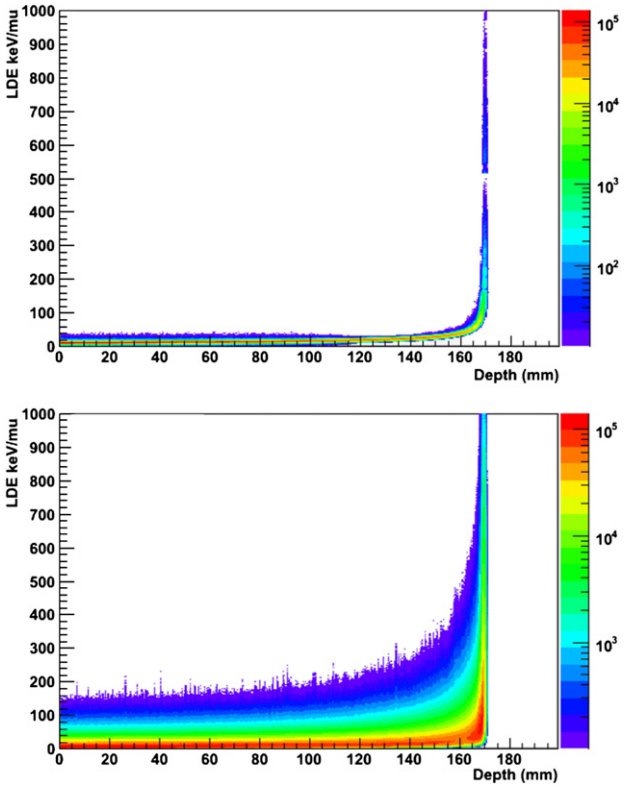

Figure 6 2D distribution of the linear deposited energy as a function of depth for two different production thresholds: 1 mm (top figure) and 10^{-3} mm (bottom figure). Each entry corresponds to the number of steps at each position.

these tables using fixed parameters, for both the range of dE/dx and the binning of this range. The range of the dE/dx table goes from 100 eV to 100 TeV with 80 logarithmic bins for the whole range. In the new Geant4.9.2 version modifications have been made on the use of physics tables and cross sections. New options have been introduced to adjust the maximum energy limits needed by the user and the binning corresponding to the selected table. We used 500 bins in a dE/dx table ranging from 100 eV to 5 GeV. We assumed that using this high resolution binning in a reduced dE/dx table range would allow better interpolation for the calculation of the cross section. These options may also modify the position of the Bragg peak. Similar tests were done to verify that the new version gives the same results as the previous one. We found that using a high resolution binning on the cross section tables allowed to observe a difference up to 0.5 mm, which is the size of the dosel used in this study, in the depth of the Bragg peak for all the tests. But the same general conclusions about the use of Geant4 parameters were reached with both versions. In a recent Beta release (Geant4 9.3-beta-01), some features concerning the stopping power tables for ions have been fixed. As for the value of the mean ionization potential of the ICRU material, data for water may change in the future versions of Geant4. One should be aware of this while using this value when a good uncertainty in the clinical range is required, as for instance in carbon ion therapy applications.

Discussion & conclusion

The aim of this work was to study the influence of production threshold and step size limit on spatial dose distribution and computation time in Geant4. Various different parameters have been investigated. We have compared the obtained c.s.d.a. ranges to the values given by the ICRU 73 report.

From the results obtained we can draw the following conclusions: First, users should not use high step size limits ($\geq$1 mm) combined with high production thresholds ($\geq$0.1 mm) even for 1D depth dose distribution. These conditions do not meet the Geant4 hypothesis of constant cross sections along the steps and may lead to large errors (greater than 2%). Second, one can use high production thresholds ($\geq$0.1 mm) combined with low step size limits ($\leq$0.1 mm) for 1D depth dose calculation. Third, the step size limit becomes non significant for low production thresholds ($\leq 10^{-2}$ mm). These parameters allow very precise simulation but drastically increase computation. Such very low values could however being useful for other applications such as micro-dosimetry.

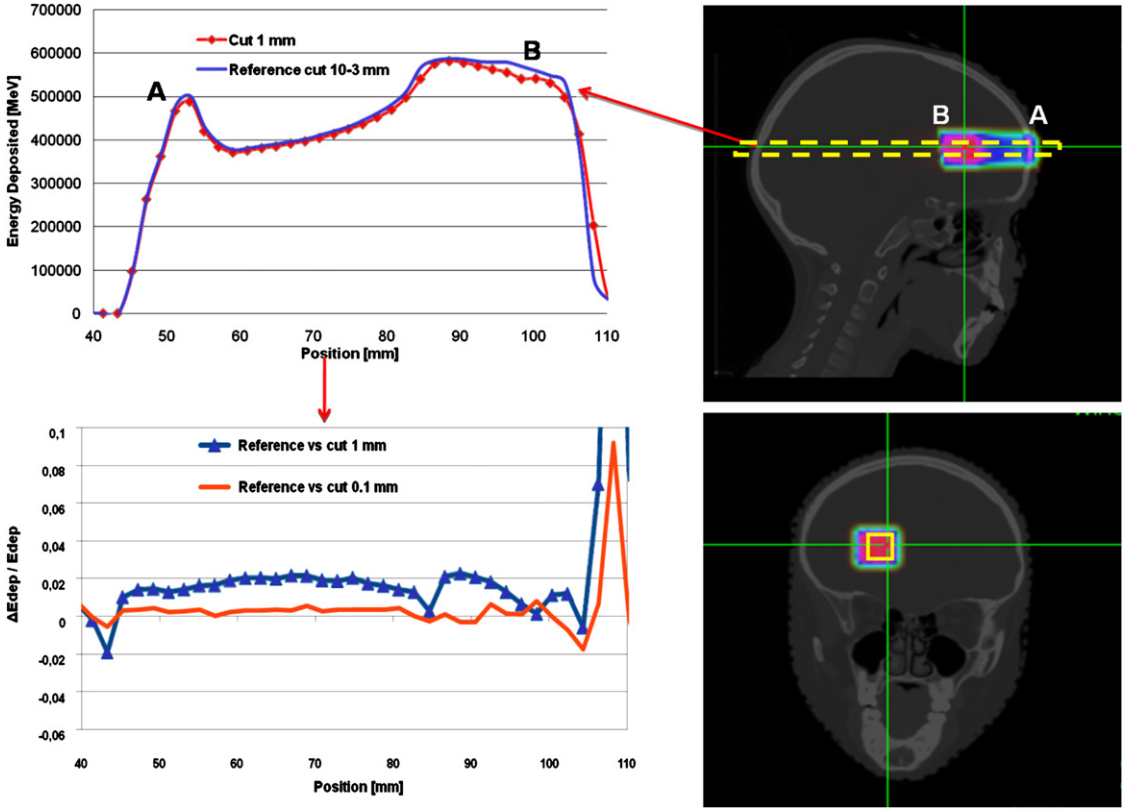

Figure 7 3D dose distributions in a cubic tumor inserted in the CT image of a patient's head using a fix step limiter and a production threshold of 10^{-3} mm. Sagital view is shown on the top right and coronal view on the bottom right. On the top left of the image we have plotted the physical energy deposited in a chosen slice of the tumor. The blue line corresponds to the reference values and triangles to a production threshold value of 1 mm. The rough variation at the 43 mm position is due to the passage from air to cortical bone ''A''. On the bottom left we show the difference in energy deposited relative to the reference. Blue triangles correspond to a production threshold of 1 mm and the red line to a production threshold of 0.1 mm. (For interpretation of the references to colour in this figure legend, the reader is referred to the web version of this article).

The best compromise found to provide accurate simulation in terms of spatial dose distribution and calculation time is the combination of a production threshold of 1 mm and a step size limit of 0.1 mm. This is valid when one is interested into millimetric dose distribution but should be tailored to other types of applications.

References

[1] Allison J, Amako K, Apostolakis J, Araujo H, Arce Dubois P, Asai M, et al. Geant4 developments and applications. IEEE Trans Nucl Sci Feb 2006;53(1):270—8.

[2] Paganetti H, Jiang H, Lee SY, Kooy HM. Accurate Monte Carlo simulations for nozzle design, commissioning and quality assurance for a proton radiation therapy facility. Med Phys Jul 2004;31(7):2107—18.

[3] Pshenichnov I, Mishustin I, Greiner W. Distributions of positron-emitting nuclei in proton and carbon-ion therapy studied with Geant4. Phys Med Biol Dec 2006;51(23):6099—112.

[4] Agostinelli S, Allison J, Amako K, Apostolakis J, Araujo H, Arce Dubois P, et al. (GEANT4 Collaboration). Geant4: a simulation toolkit. Nucl Instrum Methods, A 2003;506:250—303.

[5] Bimbot R, Geissel H, Paul H, Schinner A, Sigmund P. Technical report. Journal of the ICRU 2005;5(1). Report 73, 2005.

[6] Zahra N, Lautesse P, Guigues L, Frisson T, Sarrut D. Geant4 based simulation of carbon beam irradiation inside CT image validation with radiochromic films. In: Ion beams in biology and medicine, 11th Workshop of heavy charged particles in biology and medicine; 2007.

[7] Zahra N, Frisson T, Lautesse P, Sarrut D. Towards a new model of prediction of the optical density for radiochromic films using Monte Carlo simulations for carbon ion irradiation. In: Particle therapy co-operative group, 47th conference; 2008.

[8] IAEA. Technical reports series -398: absorbed dose determination in external beam radiotherapy: International Code of Practice for Dosimetry, Vienna; 2000.

[9] Frisson T, Zahra N, Lautesse P, Sarrut D. Monte-Carlo based prediction of radiochromic film response for hadrontherapy dosimetry. Nucl Instruments Methods Phys Res Sect A: Accelerators, Spectrometers, Detectors Associated Equipment May 2009;4.

[10] Sigmund P, Schinner A. Resolution of the frozen-charge paradox in stopping of channeled heavy ions. Phys Rev Lett Feb 2001;86(8):1486—9.

[11] Andreo Pedro. On the clinical spatial resolution achievable with protons and heavier charged particle radiotherapy beams. Phys Med Biol Jun 2009;54(11):N205—15.

[12] Schardt D, Steidl P, Krmer M, Weber U, Parodi K, Brons S. Precision bragg-curve measurements for light-ion beams in water. Technical report, GSI, Darmstadt, Germany; Rhn-Klinikum AG, Marburg, Germany; HIT, Heidelberg, Germany; 2008.

[13] Sihver L, Schardt D, Kanai T. Depth-dose distributions of high-energy carbon, oxygen and neon beams in water. Jpn J Med Phys 1998;18.

[14] Henkner Katrin, Bassler Niels, Sobolevsky Nikolai, Jkel Oliver. Monte carlo simulations on the water-to-air stopping power ratio for carbon ion dosimetry. Med Phys Apr 2009;36(4):1230—5.

[15] Jan S, Santin G, Strul D, Staelens S, Assi K, Autret D, et al. GATE: a simulation toolkit for PET and SPECT. Phys Med Biol Oct 2004;49(19):4543—61.

[16] David Sarrut, Laurent Guigues. Region-oriented CT image representation for reducing computing time of Monte Carlo simulations. Med Phys Apr 2008;35(4):1452—63.

[17] Physics reference manual. GEANT4 web page, http://geant4.cern.ch.

[18] Chetty Indrin J, Curran Bruce, Cygler Joanna E, DeMarco John J, Ezzell Gary, Faddegon Bruce A, et al. Report of the aapm task group no. 105: issues associated with clinical implementation of Monte Carlo-based photon and electron external beam treatment planning. Med Phys Dec 2007;34(12):4818—53.

[19] Walters BRB, Kawrakow I, Rogers DWO. History by history statistical estimators in the BEAM code system. Med Phys Dec 2002;29(12):2745—52.